Jamie L. Miller[1], Charles A. Hibbitts[2], and Michael T. Mellon[3]

[1]The Johns Hopkins University, Department of Earth and Planetary Sciences.

[2]The Johns Hopkins University, Applied Physics Laboratory.

[3]Cornell University, Cornell Center for Astrophysics and Planetary Science.

Corresponding author: Jamie L. Miller (jmill250@jhu.edu)

Key Points:

- $MgSO_4$, $MgCl_2$, and $CaSO_4$ migration and hydration are controlled by thermal conditions during desiccation.
- Salt migration is enhanced at elevated temperatures, an effect that is especially pronounced at the surfaces of soil samples.
- Infrared reflectance data, combined with salt concentration data, may inform us about environmental influences on the salt movement within a thin film liquid phase.

Abstract

We have measured the salt content changes of soil samples in laboratory experiments to simulate the salt and water migration that may cause duricrust formation on Mars. Although the cold, dry surface of modern Mars lacks abundant, liquid water, salts may stabilize scant liquid water as thin films through freezing point depression, allowing them to migrate along temperature and water concentration gradients driven by evaporation at the surface, and to transport salts where they precipitate and cement loose soil grains into crusts. Our work also demonstrates that spectral data complements salt content changes we measured, by showing changes in the hydration states inferred in the 1950 nm water band. We simulated salt and water migration, required in salt crust formation, in Mars analog regolith, through desiccating wet loess doped with either $MgCl_2$, $MgSO_4$, or $CaSO_4$ at a temperature range of -196 °C to 150 °C. Our experiments allowed exploring temperature and depth dependencies on water and salt behaviors in 2 cm tall cylindrical soil sample tubes. The 1000 nm to 2400 nm spectral slope and the area of the 1950 nm water band correlate with salt concentration. $MgSO_4$ exhibits the greatest migration, $CaSO_4$ hydrates with weak migration, and $MgCl_2$ migrates with moderate hydration. Spectral analysis may be useful in estimating salt and water migration, and in turn, aiding in interpreting hydrological and climatic history of the regolith of Mars.

Plain Language Summary

Duricrust, a thin layer of cohesive soil, is observed globally on Mars (Golombek et al., 2006; Mellon et al., 2000). On Earth, soil grains weld to form duricrust because of salt that migrates to the surface, mobilized by liquid water from sources such as rain and groundwater. However, Mars is cold and dry, and unlike Earth, lacks liquid water sources. If we can understand how these duricrusts formed, then we can infer something about the history of Mars climate.

We test the hypothesis that duricrust forms in dry, salty soils on Mars aided by scant water in a liquid phase, sometimes called "thin films", that occurs as a single layer of H_2O molecules attached to the surfaces of soil grains. These films are stable on cold, dry Mars and can attach to salts and move them around the soil to cohere the soil grains (Jakosky & Christensen, 1986). We perform experiments to examine water and salt migration at a range of temperatures and to investigate how salt movement and hydration changes the infrared reflectance spectra of the soil. Spectra may be used to infer information about salt abundance, water, and temperature during duricrust formation and help us to glean more information from remotely sensed spectral data on Mars.

1 Introduction

Soluble salts have long been hypothesized to exist on Mars, inferred from the aqueous history, and have been observed on Mars both in global extent and in local concentrations. Viking identified ~0.5 cm thick duricrusts with Cl- and S-rich cements (Clark et al., 1982; Clark, 1993) with 8-15 wt% sulfate (Fe,Ca,Al,Mg) and 0.5-1.5% chloride (Na,Mg,Ca,Fe) (Clark & van Hart, 1981). Phoenix measured ~1 wt% sulfate in the regolith, reported as epsomite and gypsum (Kounaves et al., 2010) and ~0.5 wt% perchlorates with trace chlorides, with Mg^{2+} and Na^{+} as dominant cations and K^{+} and Ca^{2+} as minor cations (Hecht et al, 2009). Curiosity detected gypsum veins (Nachon et al., 2014), as well as basanite and anhydrite in mudstones (Vaniman et al., 2014). The Compact Reconnaissance Imaging Spectrometer observed hydrated Mg sulfates around the rim of Endeavor crater at Meridiani Planum (Wray et al., 2009). Mars Express OMEGA mapped 5-7 wt% hydrated sulfates – kieserite, gypsum, and polyhydrated phases – at Valles Marineris using diagnostic water absorption features at 1.4, 1.9 and 2.2 m (Gendrin et al., 2005; Milliken et al., 2007). Chlorides were detected by Mars Odyssey in Terra Sirenum (Glotch et al., 2010), and globally in valley networks and basins (Osterloo et al., 2010).

The transport and deposition of these salts by water may form duricrusts, thin cohesive surface layers that result from a salt-based cementation of soil grains. Indeed, observed martian duricrusts tend to contain elevated soluble salt concentrations compared to underlying loose soil (Clark et al., 1982; Clark et al., 2005). Remote sensing observations reveal that duricrusts are globally distributed and have been inferred from correlations of albedo, thermal inertia data (Christensen & Moore, 1992; Jakosky & Christensen, 1986; Mellon et al., 2000), thought their age and origin is uncertain. Crusty, cloddy surface regolith has been excavated to reveal steep, cohesive trench slopes by Viking (Baird et al., 1977 ; Moore et al., 1987) and Phoenix (Shaw et al., 2009). The Spirit, Opportunity, and Curiosity rovers disturbed soil to reveal mm-to-cm thick cloddy, cohesive surface crusts, often with cements or coatings (Squyres et al, 2004a; Squyres et al, 2004b; Vasavada et al., 2017).

On Mars, liquid water is currently restricted to an adsorbed phase on the soil grains because of the very low absolute humidity in the pore space, which originates from an atmospheric vapor or sublimation of an underlying ice table

(Mellon et al., 1997). Thin adsorbed films (up to several nm thick) may transport salts along grain surfaces (Granick, 1991; Rodriguez-Navarro & Doehne, 1999) to aid in cementation (Clark & van Hart, 1981; Jakosky & Christensen, 1986), increase water mobility by osmotic pressure and water chemical potential (Zielinski et al., 2014), decrease water activity, and reduce evaporation (Altheide et al, 2009). As adsorbed water transitions to a vapor phase and salt concentrations exceed solution saturation, salts precipitate as salt crusts (subflorescence or efflorescence) to loosely cement soil grains (Goodall et al, 2000; Huinink et al., 2002; Veran-Tissoires et al., 2012; Yiotis et al., 2004).

In the experiments presented here, we desiccate wet salt-doped Mars-like soils over a temperature range (-196 to 150 $^{\circ}$C) to investigate the water and salt migration involved in salt crust formation. We measure desiccation driven salt concentration changes in soil samples across their vertical depths and note accompanying soil texture and spectral changes.

2 Materials and Methods

To examine the process of duricrust formation on Mars and the spectroscopic signatures of duricrust formation under differing environmental conditions, we designed a series of experiments to simulate conditions in which water and salts migrate due to evaporation at a range of temperatures. A preliminary experimental series was first performed, in which "thin disc" samples of wetted, salt-doped loess were desiccated and analyzed in order to assess potential for formation of surficial salt crusts and corresponding changes in surface spectra. The methodology and the results of these preliminary experiments are summarized in the supplementary materials. To simulate salt and water migration processes at depth, an experimental series was performed in which wetted, salt-doped loesses were packed into 2-cm acrylic tubes, which were then desiccated to remove the water. After desiccation, we measured salt concentration changes with depth and obtained reflectance spectra from which we infer changes in salt hydration state and water migration.

2.1. Sample preparation and experimental procedure

As a Mars analog soil we used Birch Hill loess from Alaska that originated from glacial outwash and aeolian redeposition (Johnson and Lorenz, 2000; Muhs et al., 2008), which proved suitable in preliminary experiments due to its grain size (<63 m), low clay content, low organic content, and high surface area (8.64 m^2/g). Soil grains are primarily silt sized (3.9 to 62.5 m), so water adsorption by clays is minimized, and contained a negligible (0.08 wt%) natural salt content. We chose salt species and concentrations consistent with Mars observations: $MgCl_2 \bullet 6H_2O$ (bischofite) (1 wt%), $MgSO_4 \bullet 7H_2O$ (epsomite) (10 wt%), and $CaSO_4 \bullet 2H_2O$ (gypsum) (10 wt%). These specific species exhibit a range of solubility and solute mobility, and thus provide for analysis of these effects. We added these salt concentrations to the loess as dehydrated-equivalent mass. Once doped with salts, we added distilled water to saturate the loess samples, and mixed them to a homogeneous muddy consistency.

We packed the wet loess into 2-cm acrylic tubes. We obtained spectra for salt-doped loesses before performing desiccation experiments to provide baseline spectra for comparison (Fig. S1). We chose not to subtract the 1950 nm absorption that exists prior to desiccation because we are interested in how it changes with desiccation and temperature, and we avoid adding noise to our normalized data. Clays show absorption features at 2200 to 2400 nm due to metal absorptions (McCord et al., 1998; McCord et al., 1999). However, grain size analyses show that clays are not a major constituent in our soil and they are equally present in all samples.

We desiccated the wet soils through five different procedures to characterize the effectiveness of these different temperature controlled processes, each of which may occur or be relevant to Mars. We performed experiments at subfreezing temperatures to compare the effect of freezing rates on salt and water migration (-196 and -20 $^{\circ}$C), and to examine salt and water migration in a modern Mars or arctic Earth environment (-20 $^{\circ}$C). We rapidly froze a sample set by fully submerging in liquid nitrogen (-196 $^{\circ}$C) for 10 minutes then desiccated them in a vacuum chamber at -20 $^{\circ}$C for seven days. We slowly froze another sample set at -20 $^{\circ}$C for three days then desiccated them in a vacuum chamber at -20 $^{\circ}$C for seven days. We performed desiccation experiments at ambient temperature (20 $^{\circ}$C) to examine salt and water migration at warm Mars and temperate Earth environments. We placed these samples in a dry nitrogen purge at room temperature for two weeks. We performed experiments at elevated temperatures to investigate salt and water migration in environments driven by hydrothermal or impact processes. We desiccated these samples in an oven (80 or 150 $^{\circ}$C) for three hours.

The 2 cm acrylic cylinders, once packed with wetted soil, were placed with bottom side flat on a Pyrex plate for desiccation, and were open to the atmosphere at both the top and the bottom of the cylinders, which allowed water to migrate out of both the top and bottom openings during desiccation in order to simulate a real-world system. Two additional test experiments were conducted to test the effects of changing the geometry of the cylinder: 1) a sample cylinder sealed on one end, and 2) a sample cylinder doubled in length (4 cm). The results of these experiments are summarized in the supplementary materials. Once completely desiccated, we removed cylinder samples from the acrylic tubes, sectioned them into four horizontal 50 mm-thick layers, noted color and textural changes, then obtained spectra and salt concentrations for each section. We obtained visible to near-infrared spectra of the surfaces of the discs after desiccation.

2.2. Salt concentration measurements

We measured bulk salt concentration in each of the horizontal layers of the cylinder samples to examine desiccation driven vertical salt migration. Soil subsamples (~0.1 g) were added to ~15 mL (for $MgCl_2$) or ~25 to 30 mL (for $MgSO_4$ and $CaSO_4$) of water to prepare solutions for measuring electrical conductance. We used an Omega CDH-287 Micro Conductivity Meter (K=0.1 glass dip cell containing two parallel platinum plates), calibrated with KCl standard solutions.

We converted electrical conductance to salt concentration by weight percent, using conversion factors of 0.5 (for $MgCl_2$) or 0.75 (for $MgSO_4$ and $CaSO_4$), constants that are consistent with those used in the literature and within the linear range as a dilute solution (Hubert & Wolkersdorfer, 2015; McCleskey et al., 2012), and using the known soil and water masses.

2.3. Spectral data acquisition

Reflectance spectra were obtained using fiber-fed reflectance spectrometers that operate in the visible to near-infrared range (350 to 2500 nm). All cylinder samples and some discs (-20 ˚C and 20 ˚C) were analyzed using an Analytical Spectral Devices (ASD) FieldSpec Pro spectrometer; while a Spectra Vista Corporation (SVC) spectrometer was used to analyze the remaining discs (-20 ˚C, 80 ˚C, 150 ˚C). We placed samples inside 2x2 inch polystyrene containers lined with aluminum foil, and used powdered polytetrafluoroethylene as a white reference standard. Matlab data processing plotted intensity and wavelength and corrected for calibration imperfections including for the spectral features in the white reference Spectralon (USGS Spectral Library). Spectra were normalized at 800 nm, the common maximum intensity for all spectral data, in order to examine changes in spectral slope from 1000 nm to 2400 nm to assess changes in apparent grain size or cementation of soil samples. The 1950 nm water absorption band was normalized to one between 1850 nm to 2050 nm, the left and right wavelength maxima respectively, in order to accurately assess changes in band shape due to changes in salt hydration state or water migration.

3 Results

The 1000-2400 nm spectral slope and band shape at 1950 nm change with temperature and soil depth (Fig. 1). For all desiccation temperatures, $MgSO_4$ spectral slopes changed the most of all the salts, with the greatest effects at the top of the soil sample surface and a slight increase in the bottom of the soil sample surface with increasing desiccation temperatures. Generally, the 1950 nm band is deepest at the uppermost sample layers, decreases with sample depth, and increases slightly at the bottommost sample layers.

For all three salts, the 1950 nm band changes the least at subfreezing temperatures, especially for $MgCl_2$ and $CaSO_4$ (Fig. 2). At -196 ˚C, the band depth is constant for $CaSO_4$, and a small shoulder is seen across layers. At -20 ˚C, the band depth does not change significantly for $CaSO_4$, and a small shoulder is seen across layers. At 20 ˚C, the band deepens for $MgCl_2$, and only slightly for $CaSO_4$. At 80 ˚C, the band deepens for $MgCl_2$. The band slightly deepens for $CaSO_4$, and the band for the top surface shifts toward a shorter wavelength and gains a small shoulder. At 150 ˚C, the band deepens notably for $MgCl_2$ and gradually deepens for $CaSO_4$. The band for the bottom section of $MgSO_4$ broadens.

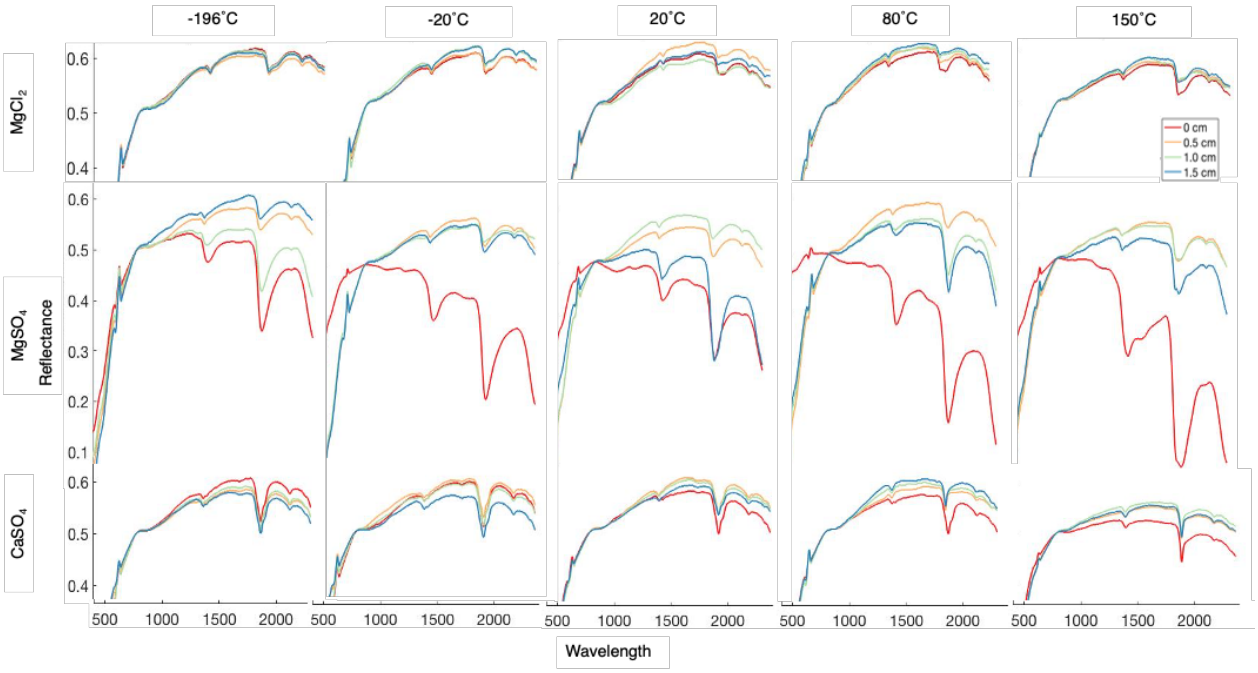

Figure 1. The 1000-2400 nm spectral slope and band shape at 1950 nm wavelength. These features change with temperature and soil depth. $MgSO_4$ spectral slopes changed drastically, with the greatest effects at the top of the soil sample surface. The 1950 nm band is deepest at the uppermost sample layers and decreases with sample depth.

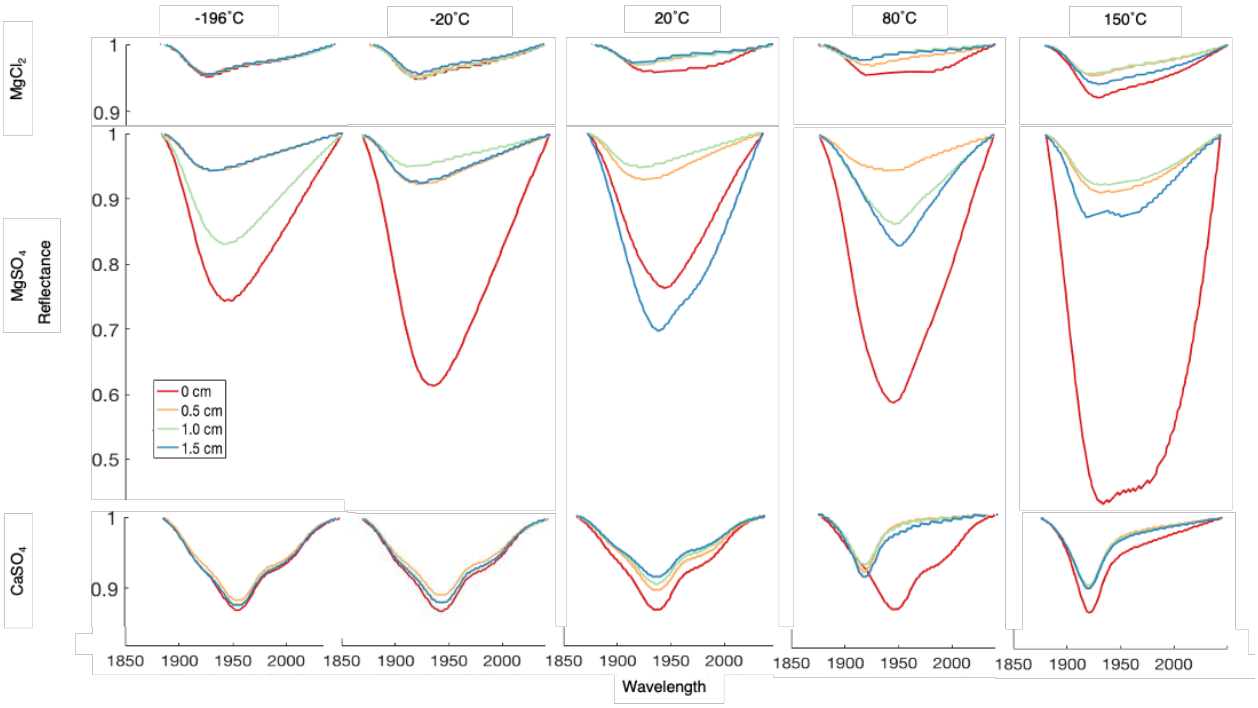

Figure 2. The 1950 nm wavelength water band. This band changes the least at subfreezing temperatures, especially for $MgCl_2$ and $CaSO_4$, and changes more with sample depth at higher temperatures.

Band area is greatest and changes more strongly with temperature in the 1950 nm band of $MgSO_4$ samples (Fig. 3). Band area is largely invariant with respect to desiccation temperatures at the surfaces of samples containing $CaSO_4$ and $MgCl_2$ salts, but do vary in samples containing $MgSO_4$ salt. For $CaSO_4$, band area decreases with increasing desiccation temperature at all soil depths, with a slight increase at 150 $^\circ$C. Trends are less clear for $MgSO_4$ and $MgCl_2$. In $MgSO_4$, band areas in deeper sample layers are fairly independent of desiccation temperature except at the surface. In $MgCl_2$, band area at the sample surface increases with temperature, while subsurface band areas decrease with temperature, then increase again at the bottom layer. The change in band area as a function of sample depth is greatest among $MgSO_4$ samples, and greatest at the sample surface for all salts and temperatures, especially for $MgSO_4$. Band area occasionally increases slightly at the sample bottom. At subfreezing temperatures, especially for $MgSO_4$ and $MgCl_2$, band areas are similar, but become more disparate with increased temperatures.

Salt concentrations vary with soil sample depth (Fig. 4). Generally, salt concentrations are highest in the uppermost (0.0 to 0.5 cm) section, and often increase in the bottommost (1.5 to 2.0 cm) section of the samples as well. $MgSO_4$ concentrations vary the greatest across depths, while $CaSO_4$ changes the least.

Only minor changes occur in salt concentrations when the sample was held at subfreezing temperatures. Interestingly, even when held at 20 ˚C, $MgCl_2$ and $CaSO_4$ do not show an increase within the 1.5 cm section, contrary to the general trend. Salt migration rates, obtained from linear regressions of salt concentrations, show that $MgCl_2$ and $CaSO_4$ are fairly constant, and that the $MgSO_4$ migration rate is highest at all temperatures.

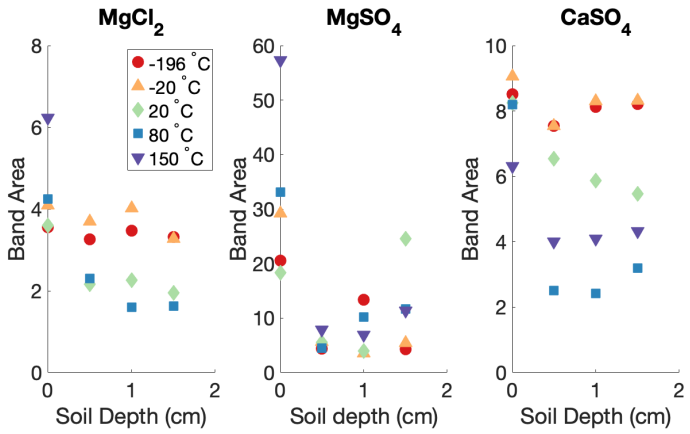

Figure 3. Band area at 1950 nm varies with soil sample depth. The top soil surface is at 0 cm and the bottom soil surface is at 2 cm. The band area is largest among $MgSO_4$ samples. Band area is largest at the top soil surface, decreases at 0.5 and 1.0 cm depths, then increases slightly again at 1.5 cm depth in most cases. The band area is fairly constant at subfreezing temperatures.

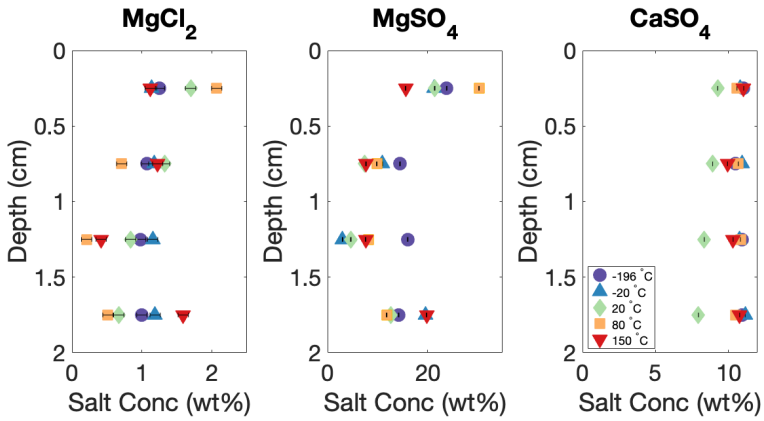

Figure 4. Salt concentration changes at soil sample depth over a range of experimental temperatures. Sample depths are measured from the uppermost surface (0 cm) to the bottommost surface (2 cm). The salt concentration is generally highest in the uppermost section (0 to 0.5 cm depth) and sometimes also at the bottommost section (1.5 to 2.0 cm depth). The salt concentration changes the most across the temperature range for $MgSO_4$ and the least for $CaSO_4$.

4 Discussion

We focus on changes in the diagnostic water absorption bands at 1400 and 1950 nm for the presence of adsorbed or structural water in our desiccated samples. These bands arise from overtones and combinations of fundamentals of the water molecule: the symmetric and asymmetric OH stretches and the HOH bend (Cloutis et al., 2006; Crowley, 1991; Hunt, 1977). The physical state of the water (frozen, liquid, adsorbed) and abundance affect the positions, shapes, number of absorption bands, band broadening and overlap (Cloutis et al., 2006; McCord et al., 1998; McCord et al., 2001). Less hydrated salts have narrower, distinct bands, and in fully dehydrated salts the water bands of course totally disappear. As water content increases, individual bands broaden and gradually merge (Cloutis et al., 2006; Crowley, 1991; Hunt, 1977; McCord et al., 1998). We observe a general trend among all salts and temperatures of a shallower band at the middle soil sample depths, and deeper bands at the top and bottom of soil sample surfaces, which correlates to water migration toward the atmosphere.

As hydrated magnesium sulfate phases are desiccated, absorption bands begin to disappear at 1950 nm (McCord et al., 1998; McCord et al., 2001). The 1200 nm band distorts to become a shoulder on the wing of the stronger 1400 nm band (McCord et al., 1999), which we observe in the upper soil sample surface layer at 150 °C. We also observe a band narrowing between 150 °C to 80 °C, which may be due to a cooler temperature causing narrower bands in a hydrated magnesium sulfate phase (McCord et al., 1998; McCord et al., 1999). For calcium sulfate, the 1950 nm band narrows at 150 °C, signaling dehydration. At 80 °C the shoulder at 1950 nm starts to disappear, first at lower soil depths, then at the surface at 150 °C. In magnesium chloride samples, we observe the 1950 nm band broaden and flatten at 20 and 80 °C as a hydrated phase, then narrow at 150 °C, signaling dehydration. Band area and depth change slightly, mostly due to the narrowing and deepening of the 1950 nm band at elevated temperatures, especially in the uppermost soil surface layer. The strongest hydration of $MgCl_2$ correlates with its migration at mid-range temperatures. $MgCl_2$ appears to have an ability to retain water in its thin film phase, as they are simultaneously hydrated and mobile.

Grain size changes overall spectral brightness and band shape by altering the distance photons travel through grains and absorption at scattering boundaries (Cloutis et al., 2006; Crowley, 1991; McCord et al., 1998). Our source soil is homogeneous and well sorted, but grains may accumulate salt coatings, making larger grains that are spectrally darker, absorb light at longer wavelengths, and have steeper spectral slopes (McCord et al., 1999; McCord et al., 2001). Cementation has been shown to produce near-IR to thermal mid-IR changes (Cooper & Mustard, 2001).

Spectral slopes and water absorption bands may be used as proxies for migration of water and hydration of salts. Spectral changes due to water may occur in two ways. First, water may migrate as vapor without transporting salts, adsorbing

to grains as it migrates or becoming incorporated into salt hydration. This effect is reflected in the water band at 1950 nm, but may not show an accompanying change in salt concentration. Second, water may migrate as a thin film or capillary phase transporting salts, with an observable change in the 1950 nm water band and changing salt hydration state, or as adsorbed water with an accompanying change in salt concentration.

Spectra correlate with changes in salt concentrations in some cases, such as at lower temperatures and for subsurface soil samples (Fig. 5). In some cases, however, salt and water migration do not correlate well, such as at higher temperatures when salt migration is very high, especially near the atmosphere. Here, the correlation for band area with salt concentration becomes disparate from the subsurface layers. For $MgCl_2$ and $CaSO_4$, which have lower mobility, band areas tightly cluster within a given temperature range, especially at lower temperatures. In $MgSO_4$, which has higher mobility, band areas cluster more loosely, spreading out at higher temperatures. For known salt concentrations, band area may provide a rough estimate for the temperature of salt precipitation; for known temperatures, salt migration may be loosely inferred with depth.

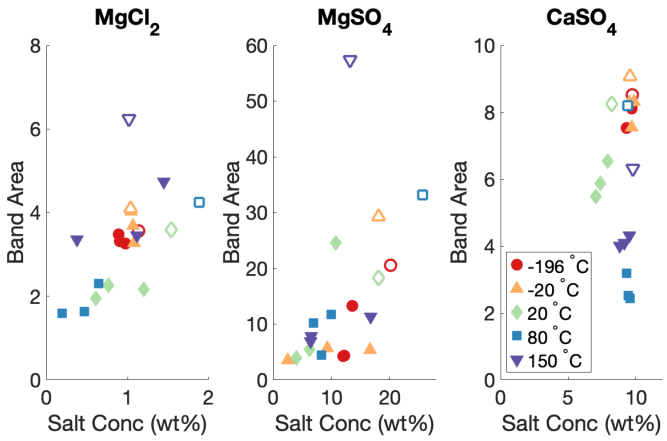

Figure 5. Band area as a proxy for salt migration. Area of the band at the 1950 nm water absorption feature is plotted against the salt concentration for each of the four horizontal sections in the 2 cm cylinder desiccation experiments. Band areas form clusters at each desiccation temperature. Tight clusters appear for lower temperatures, and spread out at higher temperatures, especially at the top surfaces (open symbols). Clusters are tighter for the weaker migrators: $MgCl_2$ and $CaSO_4$.

We focused on the migration behaviors of only single-salt species. In practice, Mars regolith contains multiple salt species of various ions and hydration states. Therefore, the quantitative results presented in this study are useful only when a single salt species is present, but serve to qualitatively illustrate potentially diagnostic remote sensing signatures. Additionally, desiccation rates vary with desiccation temperatures, and were not controlled in this study. Desiccation

times were highest for ambient experiments, and lowest for oven baked experiments. Therefore, complex rate-limiting steps, that contribute to salt migration behavior, were not addressed.

5 Conclusions

In our experiments, we examined a range of temperature effects on salt transport and crust formation using multiple salt species commonly found on Mars. $MgSO_4$ significantly migrated and hydrated, while $MgCl_2$ migrated with little change in hydration, and $CaSO_4$ migrated with significant hydration. The ability of $MgSO_4$ to incorporate more water into its structure through higher number of possible hydration states compared to $MgCl_2$, is apparent in the broadened 1950 nm water band upon hydration, especially at higher temperatures. When water migrates in an adsorbed phase, it can transport salts to change both salt concentration and hydration states, as we see in the case of $MgSO_4$ and to some extent in $MgCl_2$. When water migrates as a vapor phase, it is removed from the soil without transporting salts, so hydration occurs with less accompanied salt concentration change, as we see in $CaSO_4$. A deeper band signifies more water molecules resulting from two effects: 1) higher adsorbed water migration drives more salts to increase salt abundance, such as we observe in the top surfaces of most samples, or 2) due to more water sites available in the salt structure, or fewer water molecules at weak sites.

These results present a novel avenue for further research into remote sensing tools to investigate environments where duricrusts form on Mars. Spectral remote sensing offers insight into salt concentration and hydration states, which appear to differ between hot and cold desiccation processes. The differences in these processes should be at play during the shift from a wetter, warmer environment to a dryer, colder one. The identification of hydrated salts at a specific location may indicate the persistence of liquid water. These experiments are useful in considering data retrieved from multiple samples taken at depth. This study should motivate future mission plans to include sophisticated drilling implements, including missions to icy moons.

Acknowledgments

We owe many thanks to our colleagues who contributed their time and expertise. We thank Karen Stockstill-Cahill for her assistance in performing laboratory tasks, and Drew Knuth for support in constructing experimental apparatuses. The work was supported in part by NASA through grant NNX16AH14G. Data files are provided in http://doi.org/10.5281/zenodo.3579467.

References

Altheide, T., Chevrier, V., Nicholson, C., & Denson, J. (2009). Experimental investigation of the stability and evaporation of sulfate and chloride brines on Mars. Earth and Planetary Science Letters, 282(1), 69–78. https://doi.org/10.1016/j.epsl.2009.03.002

Baird, A. K., Castro, A. J., Clark, B. C., Toulmin III, P., Rose Jr., H., Keil, K.,

& Gooding, J. L. (1977). The Viking X Ray Fluorescence Experiment: Sampling strategies and laboratory simulations. *Journal of Geophysical Research (1896-1977)*, *82*(28), 4595–4624. https://doi.org/10.1029/JS082i028p04595

Clark, B.C., Morris, R. V., McLennan, S. M., Gellert, R., Jolliff, B., Knoll, A. H., … Rieder, R. (2005). Chemistry and mineralogy of outcrops at Meridiani Planum. *Earth and Planetary Science Letters*, *240*(1), 73–94. https://doi.org/10.1016/j.epsl.2005.09.040

Clark, Benton C. (1993). Geochemical components in Martian soil. *Geochimica et Cosmochimica Acta*, *57*(19), 4575–4581. https://doi.org/10.1016/0016-7037(93)90183-W

Clark, Benton C., Baird, A. K., Weldon, R. J., Tsusaki, D. M., Schnabel, L., & Candelaria, M. P. (1982). Chemical composition of Martian fines. *Journal of Geophysical Research: Solid Earth*, *87*(B12), 10059–10067. https://doi.org/10.1029/JB087iB12p10059

Clark, Benton C., & Van Hart, D. C. (1981). The salts of Mars. *Icarus*, *45*(2), 370–378. https://doi.org/10.1016/0019-1035(81)90041-5

Cloutis, E. A., Hawthorne, F. C., Mertzman, S. A., Krenn, K., Craig, M. A., Marcino, D., … Vilas, F. (2006). Detection and discrimination of sulfate minerals using reflectance spectroscopy. *Icarus*, *184*(1), 121–157. https://doi.org/10.1016/j.icarus.2006.04.003]

Cooper, C. D., & Mustard, J. F. (2002). Spectroscopy of Loose and Cemented Sulfate-Bearing Soils: Implications for Duricrust on Mars. *Icarus*, *158*(1), 42–55. https://doi.org/10.1006/icar.2002.6874

Crowley, J. K. (1991). Visible and near-infrared (0.4–2.5 m) reflectance spectra of Playa evaporite minerals. *Journal of Geophysical Research: Solid Earth*, *96*(B10), 16231–16240. https://doi.org/10.1029/91JB01714

Christensen, P., & Moore, H. J. (1992). The Martian surface layer. In H. H. Kieffer (Ed.), Mars (pp. 686-729). University of Arizona Press, Space Science Series.

Gendrin, A., Mangold, N., Bibring, J.-P., Langevin, Y., Gondet, B., Poulet, F., … LeMouélic, S. (2005). Sulfates in Martian Layered Terrains: The OMEGA/Mars Express View. *Science*, *307*(5715), 1587–1591. Retrieved from JSTOR.

Glotch, T. D., Bandfield, J. L., Tornabene, L. L., Jensen, H. B., & Seelos, F. P. (2010). Distribution and formation of chlorides and phyllosilicates in Terra Sirenum, Mars. *Geophysical Research Letters*, *37*(16). https://doi.org/10.1029/2010GL044557

Golombek, M. P., Grant, J. A., Crumpler, L. S., Greeley, R., Arvidson, R. E., Bell, J. F., … Squyres, S. W. (2006). Erosion rates at the Mars Exploration Rover

landing sites and long-term climate change on Mars. *Journal of Geophysical Research: Planets*, *111*(E12). https://doi.org/10.1029/2006JE002754

Goodall, T. M., North, C. P., & Glennie, K. W. (2000). Surface and subsurface sedimentary structures produced by salt crusts. *Sedimentology*, *47*(1), 99–118. https://doi.org/10.1046/j.1365-3091.2000.00279.x

Granick, S. (1991). Motions and Relaxations of Confined Liquids. Science, 253(5026), 1374–1379.

Hecht, M. H., Kounaves, S. P., Quinn, R. C., West, S. J., Young, S. M. M., Ming, D. W., … Smith, P. H. (2009). Detection of Perchlorate and the Soluble Chemistry of Martian Soil at the Phoenix Lander Site. *Science*, *325*(5936), 64–67. Retrieved from JSTOR.

Hubert, E., & Wolkersdorfer, C. (2015). Establishing a conversion factor between electrical conductivity and total dissolved solids in South African mine waters. *Water SA*, *41*(4), 490. https://doi.org/10.4314/wsa.v41i4.08

Huinink, H., Pel, L., & A. J. Michels, M. (2002). How Ions Distribute in a Drying Porous Medium: A Simple Model. *Physics of Fluids*, *14*, 1389–1395. https://doi.org/10.1063/1.1451081

Hunt, G. R. (1977). Spectral signatures of particulate minerals in the visible and near infrared. *Geophysics*, *42*(3), 501–513. https://doi.org/10.1190/1.1440721

Jakosky, B. M., & Christensen, P. R. (1986). Global duricrust on Mars: Analysis of remote-sensing data. *Journal of Geophysical Research: Solid Earth*, *91*(B3), 3547–3559. https://doi.org/10.1029/JB091iB03p03547

Johnson, J. B., & Lorenz, R. D. (2000). Thermophysical properties of Alaskan loess: An analog material for the Martian polar layered terrain? *Geophysical Research Letters*, *27*, 2769–2772. https://doi.org/10.1029/1999GL011077

Kounaves, S. P., Hecht, M. H., Kapit, J., Quinn, R. C., Catling, D. C., Clark, B. C., … Shusterman, J. (2010). Soluble sulfate in the martian soil at the Phoenix landing site. *Geophysical Research Letters*, *37*(9). https://doi.org/10.1029/2010GL042613

McCleskey, R. B., Nordstrom, D. K., & Ryan, J. N. (2012). Comparison of electrical conductivity calculation methods for natural waters: Methods for calculation of conductivity. *Limnology and Oceanography: Methods*, *10*(11), 952–967. https://doi.org/10.4319/lom.2012.10.952

McCord, T. B. (1998). Salts on Europa's Surface Detected by Galileo's Near Infrared Mapping Spectrometer. *Science*, *280*(5367), 1242–1245. https://doi.org/10.1126/science.280.5367.1242

McCord, T. B. (2001). Hydrated Salt Minerals on Ganymede's Surface: Evidence of an Ocean Below. *Science*, *292*(5521), 1523–1525. https://doi.org/10.1126/science.1059916

McCord, T. B., Hansen, G. B., Matson, D. L., Johnson, T. V., Crowley, J. K., Fanale, F. P., … Ocampo, A. (1999). Hydrated salt minerals on Europa's surface from the Galileo near-infrared mapping spectrometer (NIMS) investigation. *Journal of Geophysical Research: Planets*, *104*(E5), 11827–11851. https://doi.org/10.1029/1999JE900005

Mellon, M. T., Jakosky, B. M., Kieffer, H. H., & Christensen, P. R. (2000). High-Resolution Thermal Inertia Mapping from the Mars Global Surveyor Thermal Emission Spectrometer. *Icarus*, *148*(2), 437–455. https://doi.org/10.1006/icar.2000.6503

Mellon, M. T., Jakosky, B. M., & Postawko, S. E. (1997). The persistence of equatorial ground ice on Mars. *Journal of Geophysical Research: Planets*, *102*(E8), 19357–19369. https://doi.org/10.1029/97JE01346

Milliken, R. E., Mustard, J. F., Poulet, F., Jouglet, D., Bibring, J.-P., Gondet, B., & Langevin, Y. (2007). Hydration state of the Martian surface as seen by Mars Express OMEGA: 2. H $_2$ O content of the surface: HYDRATION STATE OF THE MARTIAN SURFACE. *Journal of Geophysical Research: Planets*, *112*(E8). https://doi.org/10.1029/2006JE002853

Moore, H. J., Hutton, R. E., Clow, G. D., & Spitzer, C. R. (1987). *Physical properties of the surface materials at the Viking landing sites on Mars* (USGS Numbered Series No. 1389). Retrieved from http://pubs.er.usgs.gov/publication/pp1389

Muhs, D. R., Ager, T. A., Skipp, G., Beann, J., Budahn, J., & McGeehin, J. P. (2008). Paleoclimatic Significance of Chemical Weathering in Loess-Derived Paleosols of Subarctic Central Alaska. *Arctic, Antarctic, and Alpine Research*, *40*(2), 396–411. https://doi.org/10.1657/1523-0430(07-022)[MUHS]2.0.CO;2

Nachon, M., Clegg, S. M., Mangold, N., Schröder, S., Kah, L. C., Dromart, G., … Wellington, D. (2014). Calcium sulfate veins characterized by ChemCam/Curiosity at Gale crater, Mars. *Journal of Geophysical Research: Planets*, *119*(9), 1991–2016. https://doi.org/10.1002/2013JE004588

Osterloo, M. M., Anderson, F. S., Hamilton, V. E., & Hynek, B. M. (2010). Geologic context of proposed chloride-bearing materials on Mars. *Journal of Geophysical Research: Planets*, *115*(E10). https://doi.org/10.1029/2010JE003613

Shaw, A., Arvidson, R. E., Bonitz, R., Carsten, J., Keller, H. U., Lemmon, M. T., … Trebi-Ollennu, A. (2009). Phoenix soil physical properties investigation. Journal of Geophysical Research: Planets, 114(E1). https://doi.org/10.1029/2009JE003455

Squyres, S. W., Arvidson, R. E., Bell, J. F., Brückner, J., Cabrol, N. A., Calvin, W., … Yen, A. (2004a). The Opportunity Rover's Athena Science Investigation at Meridiani Planum, Mars. *Science*, *306*(5702), 1698–1703. https://doi.org/10.1126/science.1106171

Squyres, S. W., Grotzinger, J. P., Arvidson, R. E., Bell, J. F., Calvin, W., Christensen, P. R., … Soderblom, L. A. (2004b). In Situ Evidence for an Ancient

Aqueous Environment at Meridiani Planum, Mars. *Science*, *306*(5702), 1709–1714. Retrieved from JSTOR.

Vaniman, D. T., Bish, D. L., Ming, D. W., Bristow, T. F., Morris, R. V., Blake, D. F., … Team, M. S. (2014). Mineralogy of a Mudstone at Yellowknife Bay, Gale Crater, Mars. *Science*, *343*(6169), 1243480. https://doi.org/10.1126/science.1243480

Vasavada, A. R., Piqueux, S., Lewis, K. W., Lemmon, M. T., & Smith, M. D. (2017). Thermophysical properties along Curiosity's traverse in Gale crater, Mars, derived from the REMS ground temperature sensor. *Icarus*, *284*, 372–386. https://doi.org/10.1016/j.icarus.2016.11.035

Veran-Tissoires, S., Marcoux, M., & Prat, M. (2012). Discrete Salt Crystallization at the Surface of a Porous Medium. *Physical Review Letters*, *108*(5). https://doi.org/10.1103/PhysRevLett.108.054502

Wray, J. J., Dobrea, E. Z. N., Arvidson, R. E., Wiseman, S. M., Squyres, S. W., McEwen, A. S., … Murchie, S. L. (2009). Phyllosilicates and sulfates at Endeavour Crater, Meridiani Planum, Mars. *Geophysical Research Letters*, *36*(21). https://doi.org/10.1029/2009GL040734

Yiotis, A. G., Boudouvis, A. G., Stubos, A. K., Tsimpanogiannis, I. N., & Yortsos, Y. C. (2004, November 1). Effect of liquid films on the drying of porous media. https://doi.org/10.1002/aic.10265

Zielinski, M. W., McGann, L. E., Nychka, J. A., & Elliott, J. A. W. (2014). Comparison of non-ideal solution theories for multi-solute solutions in cryobiology and tabulation of required coefficients. *Cryobiology*, *69*(2), 305–317. https://doi.org/10.1016/j.cryobiol.2014.08.005